catalysts

MDPI

Article

Hydrogenation of Aqueous Acetic Acid over Ru-Sn/TiO_2 Catalyst in a Flow-Type Reactor, Governed by Reverse Reaction

Yuanyuan Zhao, Kansei Konishi, Eiji Minami, Shiro Saka and Haruo Kawamoto *

Graduate School of Energy Science, Kyoto University, Kyoto 606-8501, Japan; zhao.yuanyuan.44e@st.kyoto-u.ac.jp (Y.Z.); konishi.kansei.mkagaku@gmail.com (K.K.); minami@energy.kyoto-u.ac.jp (E.M.); saka@energy.kyoto-u.ac.jp (S.S.)

* Correspondence: kawamoto@energy.kyoto-u.ac.jp; Tel.: +81-75-753-4737

Received: 1 October 2020; Accepted: 30 October 2020; Published: 2 November 2020

Abstract: Ru-Sn/TiO_2 is an effective catalyst for hydrogenation of aqueous acetic acid to ethanol. In this paper, a similar hydrogenation process was investigated in a flow-type rather than a batch-type reactor. The optimum temperature was 170 °C for the batch-type reactor because of gas production at higher temperatures; however, for the flow-type reactor, the ethanol yield increased with reaction temperature up to 280 °C and then decreased sharply above 300 °C, owing to an increase in the acetic acid recovery rate. The selectivity for ethanol formation was improved over the batch process, and an ethanol yield of 98 mol % was achieved for a 6.7 min reaction (cf. 12 h for batch) (liquid hourly space velocity: 1.23 h^{-1}). Oxidation of ethanol to acetic acid (i.e., the reverse reaction) adversely affected the hydrogenation. On the basis of these results, hydrogenation mechanisms that include competing side reactions are discussed in relation to the reactor type. These results will help the development of more efficient catalytic procedures. This method was also effectively applied to hydrogenation of lactic acid to propane-1,2-diol.

Keywords: hydrogenation; acetic acid; flow-type reactor; reverse reaction; lactic acid

1. Introduction

Bioethanol has drawn attention as a means of reducing our dependence on fossil fuels [1–5]. Currently, commercial bioethanol production involves alcoholic fermentation with yeast, which also releases two carbon atoms from glucose as CO_2 [6,7], resulting in low carbon conversion efficiency. Therefore, we have proposed a new ethanol production process based on acetic acid fermentation that can theoretically convert all carbon atoms into acetic acid [8]. Acetic acid is also a useful industrial chemical, and the global market size is 16.3 million tons in 2018 [9,10].

This new bioethanol production process consists of three steps: a hot-compressed water treatment to hydrolyze lignocellulosics, acetic acid fermentation, and hydrogenation of acetic acid [8]. This research focuses on the final acetic acid hydrogenation step. Transition metals on various supports including titania (TiO_2) and alumina (Al_2O_3) have been reported for hydrogenation of organic acids [11–17]. We have reported Pt [18] and Ru [19] supported on TiO_2 as potential hydrogenation catalysts for aqueous acetic acid to ethanol, by activating acetic acid with Lewis acid site (Ti). Ethanol was obtained with a batch-type reactor using a less expensive Ru-Sn/TiO_2 catalyst in a 98 mol % yield from 10 g/L of aqueous acetic acid under the optimum conditions of 10 MPa H_2 and 170 °C, although a long reaction time of 12 h was required [19].

The use of flow reactors for reactions on solid catalysts has many advantages over batch reactors [20–32]. Continuous flow hydrogenation has also recently been found to reduce reaction

times and improve selectivity and safety of operation [26–32]. For example, Numwong et al. [28] reported that the hydrogenation rate of polyunsaturated fatty acid methyl esters over Pd/C was 4–5 times faster in a flow-type than batch-type reactor. Durndell et al. [27] reported improved reactivity and selectivity towards C=O activation in hydrogenation of cinnamaldehyde over Pt/SiO_2. Olcay. et al. [32] investigated the hydrogenation of aqueous acetic acid with various catalysts including Ru/C using a flow reactor, and they reported that the ethanol selectivity increased by increasing the hydrogen pressure. However, the conversion of acetic acid was only about 16.6%.

In this paper, hydrogenation of aqueous acetic acid over 4wt%Ru-4wt%Sn/TiO_2 was investigated with the use of a commercially available flow type reactor system, H-Cube. The results are compared with those obtained from a batch type reactor reported in our previous paper [19]. Side reactions that compete with hydrogenation to ethanol were closely examined to better understand the reactions occurring and the role of the flow reactor. This catalytic system was also applied to hydrogenation of lactic acid to propane-1,2-diol.

2. Results and Discussion

2.1. Hydrogenation of Aqueous Acetic Acid to Ethanol in Flow Type Reactor

Hydrogenation of 10 g/L aqueous acetic acid over 4wt%Ru-4wt%Sn/TiO_2 was investigated in the temperature range of 160–320 °C with the use of a narrow column at 10 MPa, and the results are shown in Figure 1. The ethanol yield increased as the reaction temperature was increased to a maximum of 78 mol % at 280 °C. The optimum ethanol production temperature for the batch type reactor was 170 °C because gasification occurred at higher temperatures [19]; hence, the selectivity for ethanol formation over gasification was overall improved in the flow system. The reason for this improvement will be explained later. This improvement allowed for the use of a high reaction temperature of 280 °C. High ethanol yields were achieved for a short residence time of less than 1 min in the flow reactor, in contrast to the batch process that required reaction times as long as 12 h.

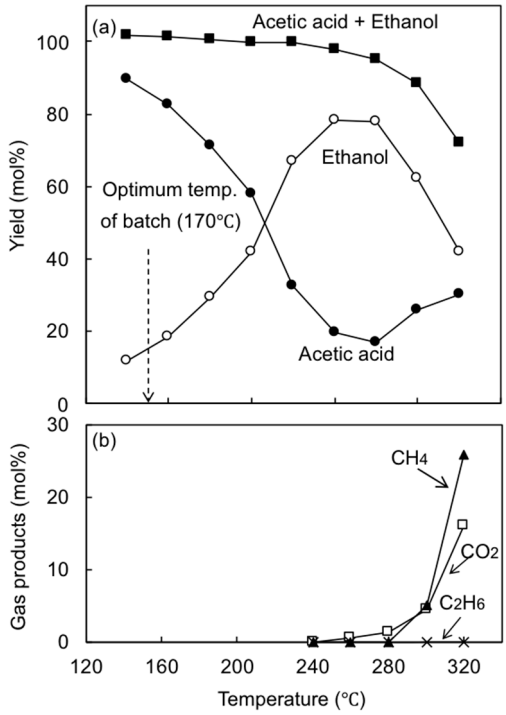

Figure 1. Effect of reaction temperature on hydrogenation of aqueous acetic acid (10 g/L) to ethanol with flow reactor: (**a**) liquid products; (**b**) gaseous products (column size: 3.9-mm inner diameter, 100-mm length; pump flow rate, 0.3 mL/min; H_2 flow rate, 60 mL/min; pressure, 10 MPa).

When the reaction temperature was higher than 300 °C, the ethanol yield sharply decreased, and the recovery rate of acetic acid increased. Thus, conversion of acetic acid to ethanol was ineffective at higher temperatures. On increasing the temperature from 300 to 320 °C, the total acetic acid + ethanol yield decreased to be 72 mol %, and gaseous products, CH_4 (26 mol %), CO_2 (17 mol %), and C_2H_6 (0.1 mol %), were the major components of the reaction mixture. Carbon dioxide started to be detected from the lower temperature at 240 °C, but CH_4 and C_2H_6 were detected above 300 °C. No carbon monoxide was detected, probably because of the occurrence of a water-gas shift reaction, as discussed later. Hydrogen might have been produced but could not be quantified because the large amount of hydrogen used in hydrogenation prevented accurate measurements. Thus, above 300 °C the ethanol yield decreased because of gasification.

Figure 2 shows the ethanol yields for acetic acid concentrations from 5 to 200 g/L at 250 °C under similar reaction conditions. The ethanol yield (mol %) decreased as the concentration increased, whereas the amount of ethanol obtained (g/L) stabilized in the range of 13–15 g/L. Thus, the acetic acid concentration was rate-determining up to this concentration but not above this range, where the amount of acetic acid converted to ethanol plateaued and was determined by the saturation capacity of the catalyst bed.

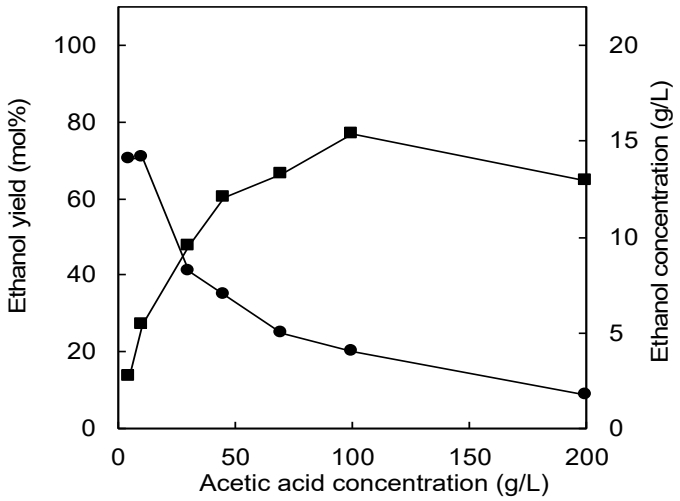

Figure 2. Effect of acetic acid concentration on ethanol yield in hydrogenation of aqueous acetic acid to ethanol at 250 °C (column size, 3.9-mm inner diameter, 100-mm length; pump flow rate, 0.3 mL/min; H_2 flow rate, 60 mL/min; pressure, 10 MPa).

The influence of H_2 on the hydrogenation of 10 g/L of acetic acid was investigated under similar reaction conditions at various H_2/AcOH molar ratios. This ratio was varied through the use of different hydrogen flow rates of 60, 36, 18, and 10 mL/min, while the aqueous acetic acid flow rate was maintained (0.3 mL/min), corresponding to H_2/AcOH molar ratios of 54:1, 32:1, 16:1, and 9:1, respectively. These ratios indicate 27:1, 16:1, 8:1, and 4.5:1 times molar in excess of the required H_2, respectively, because 2 molar equivalents of H_2 are used to reduce acetic acid to ethanol. As shown in Figure 3, this molar ratio had a limited influence on the yields of ethanol and acetic acid below 260 °C, where the results at ratios of 9:1, 16:1 and 32:1 were quite similar. Thus, the amount of H_2 is not rate-determining for hydrogenation of acetic acid to ethanol in this temperature range. Unfortunately, we could not reduce the rate further below 9 because of limitations of the leak error detector of the H-Cube reactor. Notably, 4.5 molar equivalents or less of H_2 is sufficient to reduce acetic acid to ethanol in the flow reactor, likely because of the very efficient activation of hydrogen on the catalyst surface, as will be discussed later.

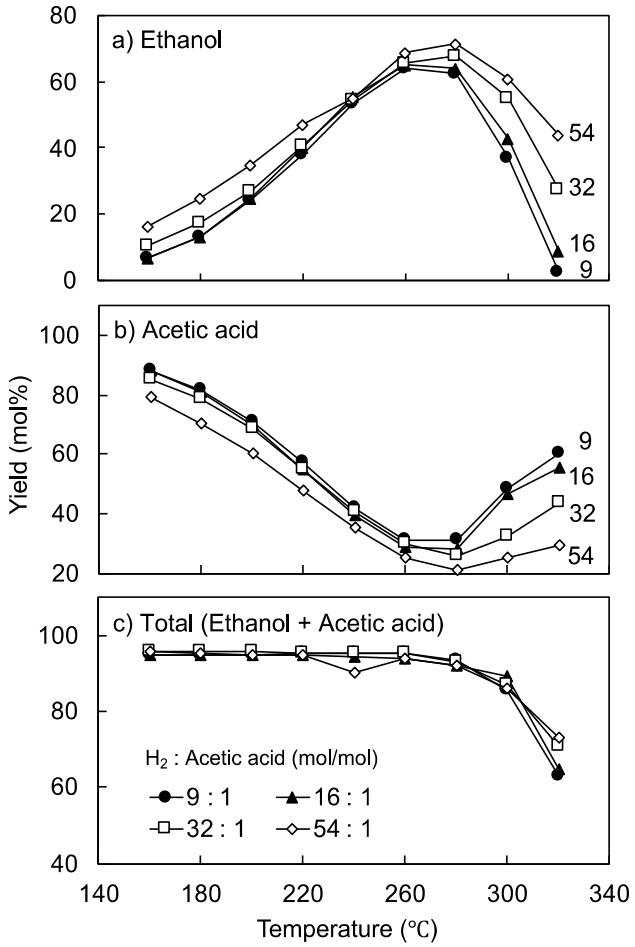

Figure 3. Effect of H_2/acetic acid ratio on hydrogenation of aqueous acetic acid (10 g/L) to ethanol: (**a**) ethanol; (**b**) acetic acid; (**c**) total (ethanol + acetic acid) (column size, 3.9-mm inner diameter, 100-mm length; pump flow rate, 0.3 mL/min, H_2 flow rate, 10–60 mL/min; pressure, 10 MPa).

Conversely, above 280 °C, the yields of ethanol and acetic acid varied greatly depending on the H_2/AcOH ratio. As previously mentioned, the ethanol yield decreased but the acetic acid recovery rate increased at higher temperatures. However, this tendency was lessened as the amount of hydrogen was increased (i.e., a higher H_2/AcOH ratio). Thus, a higher H_2/AcOH ratio was preferable for producing ethanol in this temperature range. The temperature at which the maximum ethanol yield was achieved shifted slightly to a higher range as the hydrogen content was increased.

A decrease in the total ethanol + AcOH yield was observed above 280 °C, which we attribute to gasification being slightly suppressed through the use of more hydrogen. However, the effect was smaller than those on the yields of ethanol and acetic acid as described above.

As for the stability of catalyst, once the catalyst was filled in the column, data of each Figure 1, 2, or 3 were corrected using the same catalyst column, and hence, the catalysts were utilized for long period more than 60 h. After each of the series of experiments, it was confirmed that there was no difference in catalytic activity by performing the hydrogenation under the initial test conditions. Therefore, the Ru-Sn/TiO_2 catalyst was very stable for long-term hydrogenation.

2.2. Side Reactions Competing with Ethanol Production

To understand the side reactions, aqueous ethanol and aqueous acetic acid were treated under similar reaction conditions without the use of hydrogen. The recovery rates of ethanol and acetic acid are plotted against the reaction temperature in Figure 4 and compared with the yields of gaseous products.

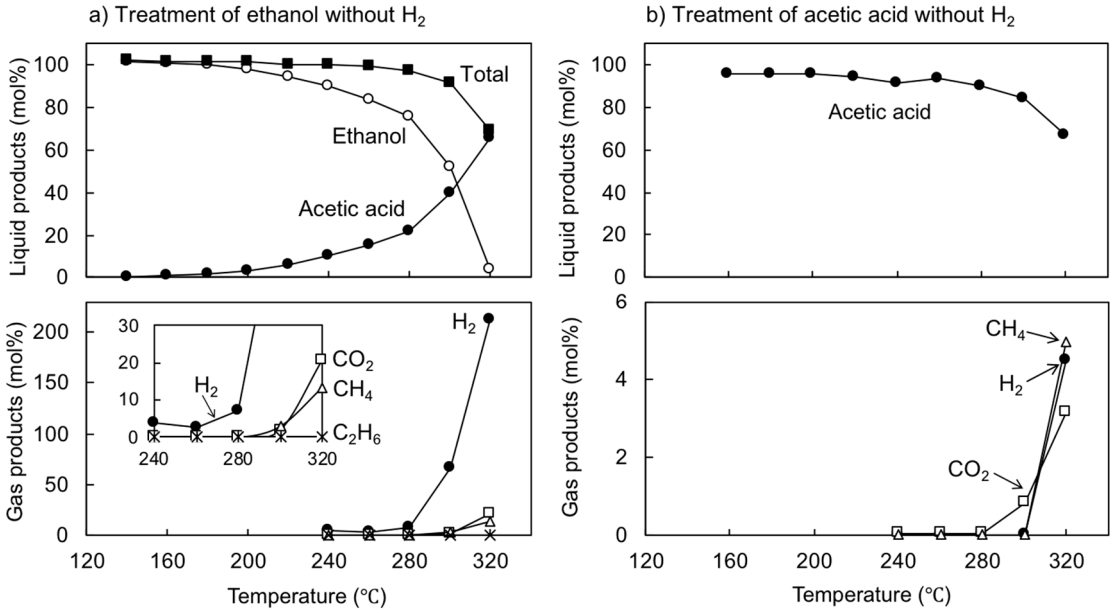

Figure 4. Product yields from treatment of aqueous (**a**) ethanol and (**b**) acetic acid (10 g/L each) without H_2 (column size, 3.9-mm inner diameter, 100-mm length; pump flow rate, 0.3 mL/min; pressure, 10 MPa).

Unexpectedly, ethanol was more reactive than acetic acid in the absence of hydrogen and converted to acetic acid at temperatures as low as 200 °C. The reaction became more pronounced above 280 °C. The total ethanol + AcOH yields of approximately 100 mol % below 280 °C suggest that oxidation reactions occurred selectively above 280 °C. Oxidation is the reverse of the hydrogenation of acetic acid to ethanol, and is thus expected to affect the apparent ethanol production rate, although this model experiment did not use any hydrogen. Inefficient conversion from acetic acid to ethanol, observed above 280 °C (Figures 1 and 3), is rationally explained by this reverse reaction. Because the efficiency of ethanol production in this temperature range is directly related to the amount of hydrogen used, the selectivity for ethanol formation rather than the reverse reaction is greater when more hydrogen used.

Large amounts of hydrogen and acetic acid were generated. The molar ratios of H_2 to AcOH in the products were 0.4:1, 0.2:1, 0.3:1, 1.7:1, and 3.2:1 at 240, 260, 280, 300, and 320 °C, respectively. Hydrogen was the only gaseous product formed in the temperature range of 240–280 °C. The simultaneous production of hydrogen and acetic acid indicates that the aqueous solvent acts as an oxidant to convert ethanol to acetic acid, although details of this mechanism are currently unknown. When water oxidizes ethanol to acetic acid, 2 equivalents of water participate in the reaction, forming 2 equivalents of hydrogen. Although the actual yields of hydrogen determined in the temperature range of 240–280 °C were lower than the theoretical value of 2, we attribute this to hydrogen being trapped in cages formed by water molecules as clathrate hydrates [33–35]. Hydrogen clathrate hydrates are known to form under high pressure conditions in water and can store up to 5 wt% hydrogen. In the current experiments, hydrogen trapped in water may not have been completely recovered during the gas-liquid separation process.

Catalytic oxidation of aqueous ethanol to acetic acid and hydrogen has also been reported in relation to reforming of ethanol to hydrogen [36–39]. In most cases, acetic acid is not the major product, whereas Nozawa et al. [38] reported that selectivity for acetic acid production is higher for Re/TiO_2 and $Ir\text{-}Re/TiO_2$ catalysts, but long reaction times were required.

The water-gas shift reaction ($CO + H_2O \rightarrow H_2 + CO_2$) has been used to explain the high yield of hydrogen from ethanol reforming [38]. This reaction also explains the high yields of hydrogen at 300 and 320 °C in the current experiments. Carbon monoxide was not detected in the present

ethanol conversion, which supports the above conclusions. A similar explanation can be made for the gas formation behavior in hydrogenation of acetic acid in Figure 1.

Treatment of acetic acid gave only gaseous products (CH_4, CO_2, and H_2) at high temperatures of 300 and 320 °C. This temperature range is similar to that for the formation of non-hydrogen gaseous products in the model ethanol experiments. Accordingly, some acetic acid and ethanol may be gasified during hydrogenation of acetic acid to ethanol; however, this effect is limited to high temperatures above 300 °C. Conversely, gas formation was observed over the lower temperature range of 240 °C in the hydrogenation of acetic acid in Figure 1. Thus, other gas formation pathways may be included in the hydrogenation of aqueous acetic acid. This topic will be discussed later in another paper.

2.3. Influences of Catalyst Column Size and Reaction Mechanism

To improve the ethanol yield, a wide column, with an inner diameter 2.4 times as wide and length 2.1 times as long as the narrow column, was used to extend the reaction time. The hydrogenation of aqueous acetic acid was conducted under similar reaction conditions to the experiments with the narrow column (Figure 1). The results from the larger column are shown in Figure 5. By increasing the reaction time to be effectively 12 times as long as for the original experiments, the conversion of acetic acid to ethanol proceeded almost completely at a relatively low temperature of 200 °C. A 98 mol % yield of ethanol was achieved even at a short residence time of 6.7 min. The liquid hourly space velocity (LHSV) was 1.23 h^{-1} (volume of the catalyst-packed region [14.6 mL] ÷ flow rate of aqueous AcOH [0.3 mL/min] × 60 min). Thus, in the continuous flow reactor, the reaction time was markedly reduced from 12 h (batch type) to 6.7 min.

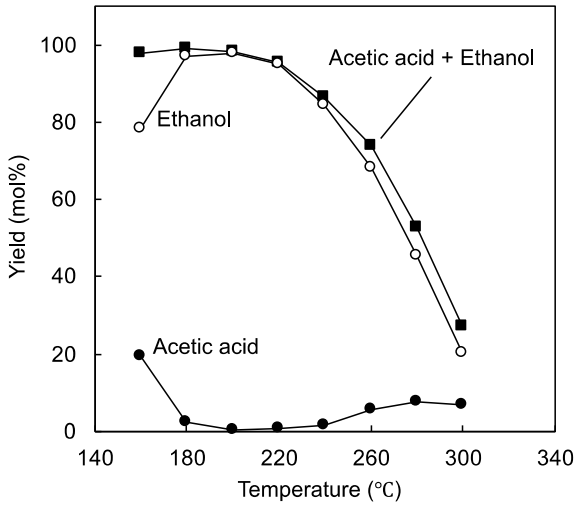

Figure 5. Effect of reaction temperature on hydrogenation of aqueous acetic acid (10 g/L) to ethanol (column size, 9.4-mm inner diameter, 210-mm length; pump flow rate, 0.3 mL/min; H_2 flow rate, 60 mL/min; pressure, 10 MPa).

The ethanol yield, however, decreased when the reaction temperature was increased beyond 200 °C. At higher temperatures, the recovery rate of acetic acid increased as was the case for the narrow column (Figures 1 and 3). Thus, the optimum temperature for ethanol production was lower in the wide column. By prolonging the reaction time up to 12 times, undesirable gasification proceeded at a lower temperature, resulting in a decrease in ethanol yield. Because the recovery of acetic acid at 200 and 220 °C was almost zero, the system was considered to be at equilibrium above 200 °C. Hence, a dynamic equilibrium was achieved between ethanol production (forward reaction) and oxidation of the product ethanol (reverse reaction).

The ethanol/acetic acid molar ratios in the reaction mixture are summarized in Table 1. The ratios obtained at 280 and 300 °C in Figure 1 (narrow column) are also included for comparison, because the

forward and reverse reactions equilibrated at the temperatures at which the acetic acid recovery rates increased. The ethanol/acetic acid molar ratios at 260, 280, and 300 °C became more similar for both types of column at higher reaction temperatures. The ratios of 3.0:1 (wide) and 2.4:1 (narrow) at 300 °C were very similar. These results indicate that the hydrogenation reaction of aqueous acetic acid to ethanol is governed by an equilibrium reaction over prolonged reaction times, where the conversion from acetic acid to ethanol is equilibrated. This is the situation for reaction temperatures higher than 240 °C (ethanol/acetic acid ratio at the equilibrium: < 49:1). Hence, 2 mol % of acetic acid contamination of ethanol occurred at 240 °C. The prolonged reaction time produced gaseous products, because gasification is an irreversible reaction.

Table 1. Ethanol/acetic acid molar ratio in the reaction mixture of hydrogenation of aqueous acetic acid (10g/L).

	Reaction Temperature (°C)					
	200	**220**	**240**	**260**	**280**	**300**
Wide column	238	120	49	12	6.1	3.0
Narrow column				3.9	4.6	2.4

Wide column: 9.4 inner diameter, 210 mm length; Narrow column: 3.9 inner diameter, 100 mm length; Reaction conditions: Pump flow rate 0.3 mL/min; H_2 flow rate 60 mL/min; pressure 10 MPa.

Table 1 shows the effects of temperature on the composition of ethanol/acetic acid at the equilibrium. The ratio varied considerably depending on the reaction temperature and the values were large at 200 °C (238:1) and 220 °C (120:1), where almost complete conversion from acetic acid to ethanol was realized through the prolonged reaction. Notably, the influence of the reaction temperature on the ratio at equilibrium was quite large compared with typical equilibrium reactions. The complex nature of the reactions, including three phases, may account for this result; however, further systematic studies are necessary to clarify the molecular based mechanisms.

Consequently, a hydrogenation mechanism of aqueous acetic acid over Ru-Sn/TiO_2 catalyst is proposed in Figure 6, in which side reactions, oxidation of the product ethanol and gasification, compete with the desired pathway to ethanol. The oxidation of ethanol (reverse reaction) greatly affects the apparent ethanol production rate above 240 °C, where the molar ratio of ethanol/acetic acid at equilibrium is <49:1. Under such high temperature conditions, the gasification reaction (an irreversible reaction) tends to govern the product composition for the prolonged reaction, although the gasification rate is much smaller than that of the ethanol-forming pathway.

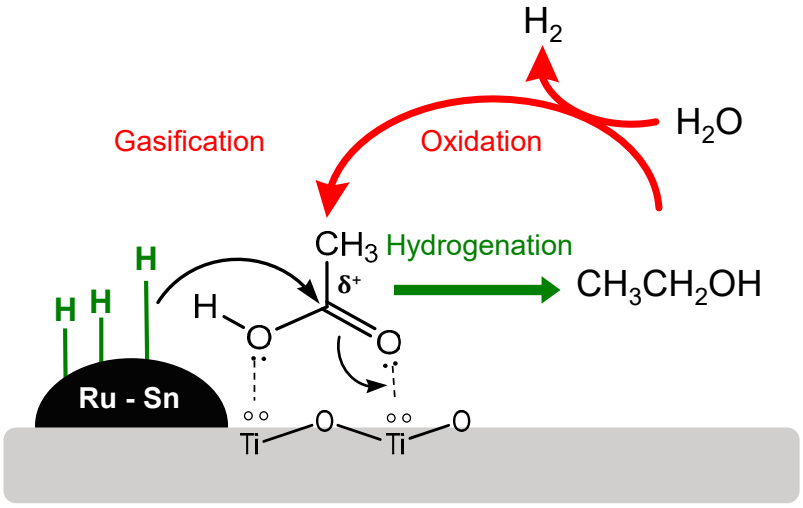

Figure 6. Proposed mechanism illustrating oxidation of the product ethanol and gasification competing with hydrogenation of aqueous acetic acid to ethanol over Ru-Sn/TiO_2 catalyst in the flow type reactor.

2.4. Roles of Flow and Batch Reactors

The characteristics of flow and batch reactors in hydrogenation are illustrated in Figure 7. In the batch reactor (a), H_2 gas is present in the upper part, and the catalyst powder sinks into the aqueous acetic acid solution. Even when the reaction system is agitated by a stirrer, contact between the H_2 gas and the catalyst is limited. There are fewer activated hydrogen atoms on the Ru-Sn surface, which limits hydrogenation of acetic acid and promotes oxidation of the product ethanol. The competition between hydrogenation and oxidation likely explains the long reaction time (12 h) required by the batch reactor in our previous study [19]. The low optimum temperature (170 °C) is also attributed to gasification becoming more prominent for long treatments and higher temperatures.

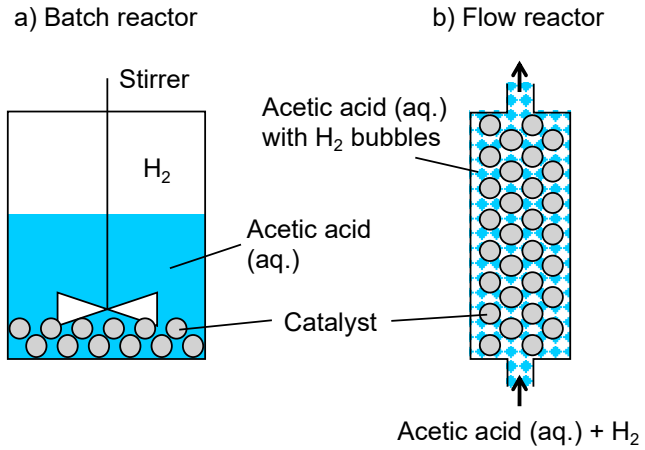

Figure 7. Difference in contact behaviors between H_2 (gas), aqueous acetic acid (liquid), and catalyst (solid) in batch and flow reactors.

In the flow reactor (b), aqueous acetic acid solution and H_2 microbubbles were continuously supplied and passed through the catalyst packed region. Therefore, H_2 gas had more contact with the catalyst surface than in the batch reactor. Thus, we expect that more activated hydrogen atoms are present on Ru-Sn for hydrogenation of acetic acid, and oxidation of ethanol is suppressed. This mechanism could explain why a very short reaction time was realized in the flow reactor. The short reaction time also suppressed the effects of gasification.

2.5. Hydrogenation of Lactic Acid to Propane-1,2-diol

In addition to acetic acid, various biomass-based organic acids produced by microbial fermentation of sugars are used in industry, and lactic acid is one of the most widely produced organic acids [40]. Propane-1,2-diol is produced by hydrogenation of lactic acid or its esters as an industrial chemical that is used as a solvent for the production of unsaturated polyester resins, drugs, cosmetics and food, de-icing fluid, and antifreeze [41–43].

The present method was applied to hydrogenation of aqueous lactic acid (10 g/L) with the use of 4wt%Ru-4wt%Sn/TiO_2 in the narrow column at 10 MPa, 250 °C, and a flow rate of 0.3 mL/min (Figure 8). As a result, propane-1,2-diol was obtained in 87 mol % yield and no other products were detected in the reaction mixture. Thus, lactic acid is efficiently hydrogenated from propane-1,2-diol in this system with a very short mean residence time of 0.5 min. Hydrogenation of lactic acid proceeded more efficiently than that of acetic acid, which is attributed to intramolecular hydrogen bonding of the former that increases polarization of the carbonyl group and enhances the hydrogenation reactivity. Efficient hydrogenation of acetic acid catalyzed by Ru-Sn/TiO_2 has been shown to be due to the binding of Ti (Lewis acid site) to the carbonyl oxygen of acetic acid, enhancing the δ+ character of the carbonyl carbon [18,19]. The carbonyl carbon of lactic acid is already activated by the intramolecular hydrogen bond. Although many papers report the hydrogenation of lactic acid [44–47] and lactate

esters [42], the present hydrogenation system with a flow reactor provides a method for efficiently producing propane-1,2-diol with a short residence time.

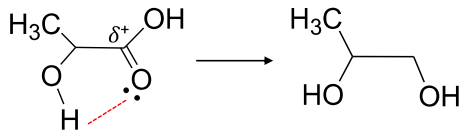

Figure 8. Hydrogenation of lactic acid to propane-1,2-diol.

Consequently, the present flow type hydrogenation system can be applied for production of alcohols from organic acids.

3. Experimental

3.1. Materials and Catalyst Preparation

Titanium isopropoxide (>95% purity), tin (II) chloride dihydrate ($SnCl_2 \cdot 2H_2O$, >97%), sodium hydroxide (NaOH, >97%), 2-propanol (>99%), and hydrochloric acid (HCl, 6 mol/L) were used for catalyst preparation. Acetic acid (AcOH, >99%) and ethanol (EtOH, >99.5%) were used for the preparation of the aqueous solutions for hydrogenation. All the above reagents were purchased from Nacalai Tesque, Inc., Kyoto, Japan. Ruthenium (III) chloride ($RuCl_3$) was provided by Tokyo chemical industry, Co. Ltd., Tokyo, Japan, and hydrogen (H_2, >99.9%) was provided by Imamura Sanso, Co. Ltd., Shiga, Japan.

In our previous study [19], the addition of Sn to 4wt% Ru/TiO_2 significantly improved the ethanol selectivity against gasification, and the Sn loading level of 4 wt% against TiO_2 was found to be optimal for the ethanol production from aqueous acetic acid. Therefore, 4wt%Ru-4wt%Sn/TiO_2 catalyst was selected and prepared by a sol-gel sedimentation method. A mixture of tetraisopropoxide and isopropanol was added dropwise to an aqueous solution of $RuCl_3$ and $SnCl_2$ at 60 °C. After the additional agitation for 30 min, aqueous NaOH solution (100 mL, with sufficient concentration for neutralizing metal chlorides) was added and stirred for 0.5 h. During this period, $RuCl_3$ and $SnCl_2$ were converted to $Ru(OH)_3$ and $Sn(OH)_2$, respectively, and then deposited on the TiO_2 surface. The reaction mixture was allowed to stand for 12 h. The obtained precipitates were washed with water fiver times and then oven-dried at 105 °C for overnight. The obtained solid was calcinated at 450 °C under an air flow (100 mL/min) for 1 h and then reduced at 400 °C under a H_2 flow (100 mL/min) for 2 h. The prepared catalysts (BET surface area = 80 ± 5 m^2/g) were adjusted to a powder with an average size of 50–70 μm for packing into the catalyst column.

3.2. Hydrogenation with Flow Type Reactor

Figure 9 shows the configuration of the flow-type reactor consisting of a flow reactor system (H-Cube Pro™, ThalesNano Inc., Budapest, Hungary) and an electric furnace (Phoenix, ThalesNano Inc., Budapest, Hungary) [48]. The system allows for a reaction pressure and temperature up to 10 MPa and 450 °C. For the hydrogenation reaction, aqueous acetic acid solution (10 g/L) was fed by a high-pressure pump at a flow rate of 0.3 mL/min, and hydrogen (H_2 > 99.9%) was mixed as microbubbles through a mixer filter. The H_2 flow rate was controlled with a mass flow controller (Gas module, ThalesNano Inc., Budapest, Hungary) at 60 mL/min. The flow rates were based on the standard ambient temperature and pressure (SATP). The mixture was preheated through a heat exchanger and supplied to a packed-bed catalyst column (4wt%Ru-4wt%Sn/TiO_2) heated at a designated temperature between 160–380 °C. The resulting mixture was then cooled by the heat exchanger. The inner pressure of the reaction system was maintained at 10 MPa by a back-pressure regulator. After the pressure was released, the reaction mixture was separated into liquid and gaseous products with a liquid-gas separator and collected in a glass bottle and a gas bag, respectively. To ensure that the reaction reached a steady state, the products were collected at least 45 min after starting to operate the system under the specified conditions.

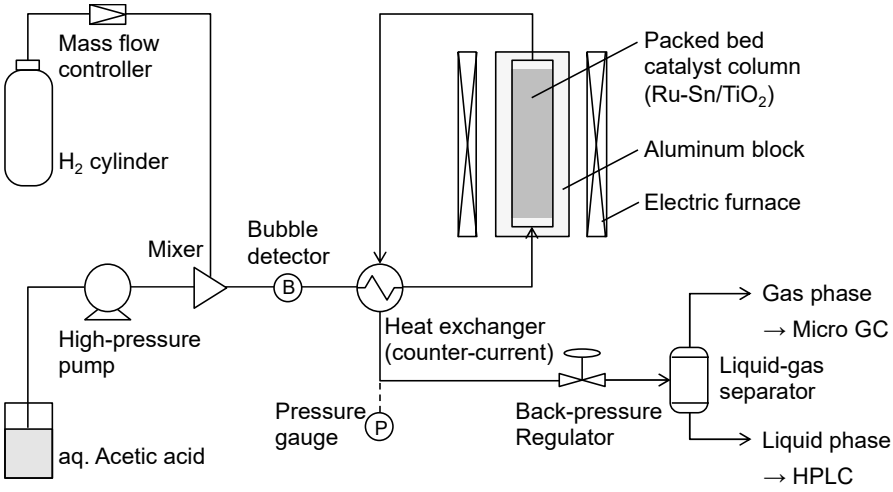

Figure 9. A flow-type reactor used for hydrogenation of aqueous acetic acid to ethanol.

The typical reaction conditions described above were altered according to the purpose of the experiment. We used two types of catalyst columns: a narrow column (inner diameter, 3.9 mm; catalyst-packed length, 100 mm) and wide column (inner diameter, 9.4 mm; catalyst-packed length, 210 mm). The porosity φ of the catalyst-packed region was 0.66 as measured by filling with water.

The mean residence time t was calculated by the following equation:

$$t = \frac{\varphi V}{F_{Aq}\frac{\rho Aq}{\rho' Aq} + F_{H_2}\frac{\rho H_2}{\rho' H_2}}, \quad (1)$$

where V is the volume of the catalyst-packed region, F is the flow rate, ρ and ρ′ are densities at SATP and reaction conditions, respectively. The subscripts Aq and H_2 correspond to aqueous acetic acid and H_2, respectively. Density changes for the acetic acid solution and H_2 were estimated with the Soave–Redlich–Kwong model that runs on a steady-state process simulator, Pro/II version 10.1 (Schneider Electric, Rueil–Malmaison, France). Under the above typical conditions, the mean residence times in the narrow column were estimated to be 0.59 min at 160 °C, 0.47 min at 280 °C, and 0.09 min at 380 °C. The reason for the short residence time at 380 °C is that at 10 MPa, water vaporizes at approximately 310 °C. Because the inner volume of the wide column was approximately 12 times that of narrow column; the residence time was 12 times as long.

3.3. Product Determination

The liquid products collected from the flow type reactor were analyzed by high-performance liquid chromatography (HPLC, LC 20 system, Shimadzu Corporation, Kyoto, Japan) under the following conditions: column, Aminex HPX-87H (300 × 7.8 mm, Bio-Rad Laboratories, Inc., Hercules, CA, USA); eluent, 5 mM sulfuric acid in water; flow-rate, 0.6 mL/min; column temperature, 45 °C; detector, refractive index detector (RID-20A, Shimadzu Corporation, Kyoto, Japan).

The gaseous products collected from the liquid-gas separator were analyzed with a micro gas chromatograph (Micro GC, CP 4900, Varian Medical Systems, Inc., Palo Alto, CA, USA), (Molsieve 5 A 10 m Column, PoraPLOT Q 10m Column, analysis time 120 s, pressure 550 ± 10 kPa, temperature 100 °C). Neon (Ne) was used as an internal standard for quantification.

4. Conclusions

Hydrogenation of aqueous acetic acid (10 g/L) over 4wt%Ru-4wt%Sn/TiO_2 was investigated with a continuous flow type reactor at 10 MPa and 160–320 °C, and the following conclusions were obtained:

1. Selectivity of the acetic acid formation against gasification was markedly improved in the flow reactor, which enabled the reaction at higher temperatures. For this reason, ethanol was obtained in 78 and 98 mol % yields at 280 and 200 °C for short residence times of 0.5 and 6.7 min (LHSV: 15.1^{-1} and 1.23 h^{-1}), respectively, (batch type: 12 h).
2. Oxidation of the product ethanol to acetic acid (reverse reaction) with water as an oxidant occurred as a side reaction, which decreased the apparent rate of ethanol production.
3. The hydrogenation of aqueous acetic acid was governed by equilibrium reactions, and hence, the ethanol/acetic acid molar ratio did not change for the prolonged reaction. This limited the reaction temperature to less than 240 °C, for which the ethanol/acetic acid molar ratio at equilibrium was 49 thus giving complete conversion of acetic acid to ethanol.
4. The ethanol/acetic acid molar ratio at equilibrium varied from 238:1 to 3.0:1 depending on the reaction temperature (from 200 to 300 °C).
5. Prolonged reactions above 240 °C gave gaseous product because gasification is irreversible. Conversely, the amount of acetic acid converted to ethanol was determined by an equilibrium process.
6. The use of a flow reactor is advantageous for the efficient activation of hydrogen and increases the rate of hydrogenation of acetic acid to ethanol rather than the reverse reaction. Thus, conversion to ethanol is completed before gasification reactions start to affect the yield.
7. Lactic acid was also reduced selectively to propane-1,2-diol in an 87 mol % yield with a residence time less than 0.5 min.
8. A hydrogenation mechanism is proposed, providing insights into the development of efficient hydrogenation catalysts and reaction systems.

Author Contributions: Formal analysis, writing—original draft preparation, investigation, data curation, Y.Z.; data curation, K.K.; data curation, writing—review and editing, supervision, E.M.; funding acquisition, supervision, S.S.; writing—review and editing, supervision, H.K. All authors have read and agreed to the published version of the manuscript.

Funding: This research was funded by Advanced Low Carbon Technology Research and Technology Development program (ALCA), grant number JPMJAL1012 supported by the Japan Science and Technology Agency (JST).

Acknowledgments: This work has been conducted since 2011 as a project of the Advanced Low Carbon Technology Research and Technology Development program (ALCA) supported by the Japan Science and Technology Agency (JST), which is highly appreciated. We thank Andrew Jackson, from Edanz Group (https://en-author-services.edanzgroup.com/ac) for editing a draft of this manuscript.

Conflicts of Interest: The authors declare no conflict of interest.

References

1. Urry, J. The problem of energy. *Theory Cult. Soc.* **2014**, *31*, 3–20. [CrossRef]
2. Kim, S.; Dale, B.E. Global potential bioethanol production from wasted crops and crop residues. *Biomass Bioenergy* **2004**, *26*, 361–375. [CrossRef]
3. Dodić, S.N.; Popov, S.D.; Dodić, J.M.; Ranković, J.A.; Zavargo, Z.Z. Potential contribution of bioethanol fuel to the transport sector of Vojvodina. *Renew. Sustain. Energy Rev.* **2009**, *13*, 2197–2200. [CrossRef]
4. Owusu, P.A.; Asumadu-Sarkodie, S. A review of renewable energy sources, sustainability issues and climate change mitigation. *Cogent Eng.* **2016**, *3*, 1–14. [CrossRef]
5. Yang, Y.; Bae, J.; Kim, J.; Suh, S. Replacing gasoline with corn ethanol results in significant environmental problem-shifting. *Environ. Sci. Technol.* **2012**, *46*, 3671–3678. [CrossRef]
6. Takagi, M.; Abe, S.; Suzuki, S.; Emert, G.; Yata, N. A method for production of alcohol directly from cellulose using cellulase and yeast. *Chem. Microb. Protein* **1977**, 551–571.
7. Schell, D.J.; Hinman, N.D.; Wyman, C.E.; Werdene, P.J. Whole broth cellulase production for use in simultaneous saccharification and fermentation. *Appl. Biochem. Biotechnol.* **1990**, *24*, 287–297. [CrossRef]
8. Saka, S.; Rabemanolontsoa, H.; Minami, E.; Kawamoto, H. Advanced ethanol production with acetic acid fermentation from lignocellulosics. *J. Jpn. Pet. Inst.* **2019**, *62*, 199–204. [CrossRef]

9. Le Berre, C. Acetic acid. *Eur. Chem. News.* **2001**, *74*, 20.
10. Dimian, A.C.; Kiss, A.A. Novel energy efficient process for acetic acid production by methanol carbonylation. *Chem. Eng. Res. Des.* **2020**, *159*, 1–12. [CrossRef]
11. Besson, M.; Gallezot, P.; Pinel, C. Conversion of biomass into chemicals over metal catalysts. *Chem. Rev.* **2014**, *114*, 1827–1870. [CrossRef]
12. Cheah, K.Y.; Tang, T.S.; Mizukami, F.; Niwa, S.I.; Toba, M.; Choo, Y.M. Selective hydrogenation of oleic acid to 9-octadecen-1-ol: Catalyst preparation and optimum reaction conditions. *J. Am. Oil Chem. Soc.* **1992**, *69*, 410–416. [CrossRef]
13. Chen, L.; Li, Y.; Zhang, X.; Zhang, Q.; Wang, T.; Ma, L. Mechanistic insights into the effects of support on the reaction pathway for aqueous-phase hydrogenation of carboxylic acid over the supported Ru catalysts. *Appl. Catal. A Gen.* **2014**, *478*, 117–128. [CrossRef]
14. Mendes, M.J.; Santos, O.A.A.; Jordão, E.; Silva, A.M. Hydrogenation of oleic acid over ruthenium catalysts. *Appl. Catal. A Gen.* **2001**, *217*, 253–262. [CrossRef]
15. Zhang, S.; Duan, X.; Ye, L.; Lin, H.; Xie, Z.; Yuan, Y. Production of ethanol by gas phase hydrogenation of acetic acid over carbon nanotube-supported Pt-Sn nanoparticles. *Proc. Catal. Today* **2013**, *215*, 260–266. [CrossRef]
16. Tahara, K.; Nagahara, E.; Itoi, Y.; Nishiyama, S.; Tsuruya, S.; Masai, M. Liquid-phase hydrogenation of carboxylic acid on supported bimetallic Ru-Sn-alumina catalysts. *Appl. Catal. A Gen.* **1997**, *154*, 75–86. [CrossRef]
17. Wan, H.; Chaudhari, R.V.; Subramaniam, B. Aqueous phase hydrogenation of acetic acid and its promotional effect on p-cresol hydrodeoxygenation. *Energy Fuels* **2013**, *27*, 487–493. [CrossRef]
18. Kawamoto, H.; Fujii, T.; Ito, Y.; Saka, S. Effects of different solvents on hydrogenation of acetic acid over Pt/TiO_2 for bioethanol production. *J. Jpn. Inst. Energy* **2016**, *95*, 162–166. [CrossRef]
19. Ito, Y.; Kawamoto, H.; Saka, S. Efficient and selective hydrogenation of aqueous acetic acid on $Ru\text{-}Sn/TiO_2$ for bioethanol production from lignocellulosics. *Fuel* **2016**, *178*, 118–123. [CrossRef]
20. Hessel, V.; Löb, P.; Krtschil, U.; Löwe, H. Microstructured reactors for development and production in pharmaceutical and fine chemistry. In *Synthesis New Avenues to Efficient Chemical Synthesis*; Seeberger, P.H., Blume, T., Eds.; Springer: Berlin/Heidelberg, Germany, 2007; pp. 205–240.
21. Roberge, D.M.; Zimmermann, B.; Rainone, F.; Gottsponer, M.; Eyholzer, M.; Kockmann, N. Microreactor technology and continuous processes in the fine chemical and pharmaceutical industry: Is the revolution underway? *Org. Process. Res. Dev.* **2008**, *12*, 905–910. [CrossRef]
22. Roberge, D.M.; Bieler, N.; Mathier, M.; Eyholzer, M.; Zimmermann, B.; Barthe, P.; Guermeur, C.; Lobet, O.; Moreno, M.; Woehl, P. Development of an industrial multi-injection microreactor for fast and exothermic reactions—Part II. *Chem. Eng. Technol.* **2008**, *31*, 1155–1161. [CrossRef]
23. Hessel, V. Novel process windows-gates to maximizing process intensification via flow chemistry. *Chem. Eng. Technol.* **2009**, *32*, 1641. [CrossRef]
24. Wiles, C.; Watts, P. Continuous flow reactors: A perspective. *Green Chem.* **2012**, *14*, 38–54. [CrossRef]
25. Hartman, R.L.; McMullen, J.P.; Jensen, K.F. Deciding whether to go with the flow: Evaluating the merits of flow reactors for synthesis. *Angew. Chem. Int. Ed.* **2011**, *50*, 7502–7519. [CrossRef] [PubMed]
26. Yu, T.; Jiao, J.; Song, P.; Nie, W.; Yi, C.; Zhang, Q.; Li, P. Recent progress in continuous-flow hydrogenation. *ChemSusChem* **2020**, *13*, 2876–2893. [CrossRef]
27. Durndell, L.J.; Wilson, K.; Lee, A.F. Platinum-catalysed cinnamaldehyde hydrogenation in continuous flow. *RSC Adv.* **2015**, *5*, 80022–80026. [CrossRef]
28. Numwong, N.; Luengnaruemitchai, A.; Chollacoop, N.; Yoshimura, Y. Partial hydrogenation of polyunsaturated fatty acid methyl esters over Pd/activated carbon: Effect of type of reactor. *Chem. Eng. J.* **2012**, *210*, 173–181. [CrossRef]
29. Gómez-Quero, S.; Cárdenas-Lizana, F.; Keane, M.A. Liquid phase catalytic hydrodechlorination of 2,4-dichlorophenol over Pd/Al_2O_3: Batch vs. continuous operation. *Chem. Eng. J.* **2011**, *166*, 1044–1051. [CrossRef]
30. Wang, Y.; Prinsen, P.; Triantafyllidis, K.S.; Karakoulia, S.A.; Yepez, A.; Len, C.; Luque, R. Batch versus continuous flow performance of supported mono- and bimetallic nickel catalysts for catalytic transfer hydrogenation of furfural in isopropanol. *ChemCatChem* **2018**, *10*, 3459–3468. [CrossRef]

31. Osako, T.; Torii, K.; Hirata, S.; Uozumi, Y. Chemoselective continuous-flow hydrogenation of aldehydes catalyzed by platinum nanoparticles dispersed in an amphiphilic resin. *ACS Catal.* **2017**, *7*, 7371–7377. [CrossRef]
32. Olcay, H.; Xu, Y.; Huber, G.W. Effects of hydrogen and water on the activity and selectivity of acetic acid hydrogenation on ruthenium. *Green Chem.* **2014**, *16*, 911–924. [CrossRef]
33. Sloan, E.D.; Koh, C.A. Molecular structures and similarities to ice. In *Clathrate Hydrates of Natural Gases*, 3rd ed.; Sloan, E.D., Ed.; CRC Press: Boca Raton, FL, USA, 2007; pp. 45–102.
34. Mao, W.L.; Mao, H.K. Hydrogen storage in molecular compounds. *Proc. Natl. Acad. Sci. USA* **2004**, *101*, 708–710. [CrossRef]
35. Ziparo, C.; Giannasi, A.; Ulivi, L.; Zoppi, M. Raman spectroscopy study of molecular hydrogen solubility in water at high pressure. *Int. J. Hydrog. Energy* **2011**, *36*, 7951–7955. [CrossRef]
36. Diagne, C.; Idriss, H.; Kiennemann, A. Hydrogen production by ethanol reforming over Rh/CeO_2-ZrO_2 catalysts. *Catal. Commun.* **2002**, *3*, 565–571. [CrossRef]
37. Xiong, H.; DeLaRiva, A.; Wang, Y.; Datye, A.K. Low-temperature aqueous-phase reforming of ethanol on bimetallic PdZn catalysts. *Catal. Sci. Technol.* **2015**, *5*, 254–263. [CrossRef]
38. Nozawa, T.; Yoshida, A.; Hikichi, S.; Naito, S. Effects of Re addition upon aqueous phase reforming of ethanol over TiO_2 supported Rh and Ir catalysts. *Int. J. Hydrog. Energy* **2015**, *40*, 4129–4140. [CrossRef]
39. Nozawa, T.; Mizukoshi, Y.; Yoshida, A.; Naito, S. Aqueous phase reforming of ethanol and acetic acid over TiO_2 supported Ru catalysts. *Appl. Catal. B Environ.* **2014**, *146*, 221–226. [CrossRef]
40. Sauer, M.; Porro, D.; Mattanovich, D.; Branduardi, P. Microbial production of organic acids: Expanding the markets. *Trends Biotechnol.* **2008**, *26*, 100–108. [CrossRef]
41. Vaidya, U.R.; Nadkarni, V.M. Unsaturated polyester resins from poly (ethylene terephthalate) waste. 1. synthesis and characterization. *Ind. Eng. Chem. Res.* **1987**, *26*, 194–198. [CrossRef]
42. Luo, G.; Yan, S.; Qiao, M.; Zhuang, J.; Fan, K. Effect of tin on Ru-B/γ-Al_2O_3 catalyst for the hydrogenation of ethyl lactate to 1,2-propanediol. *Appl. Catal. A Gen.* **2004**, *275*, 95–102. [CrossRef]
43. Fiume, M.M.; Bergfeld, W.F.; Belsito, D.V.; Hill, R.A.; Klaassen, C.D.; Liebler, D.; Marks, J.G.; Shank, R.C.; Slaga, T.J.; Snyder, P.W.; et al. Safety assessment of propylene glycol, tripropylene glycol, and PPGs as used in cosmetics. *Int. J. Toxicol.* **2012**, *31*, 245S–260S. [CrossRef]
44. Luo, G.; Yan, S.; Qiao, M.; Fan, K. Effect of promoters on the structures and properties of the RuB/γ-Al_2O_3 catalyst. *J. Mol. Catal. A Chem.* **2005**, *230*, 69–77. [CrossRef]
45. Zhang, Z.; Jackson, J.E.; Miller, D.J. Aqueous-phase hydrogenation of lactic acid to propylene glycol. *Appl. Catal. A Gen.* **2001**, *219*, 89–98. [CrossRef]
46. Broadbent, H.S.; Campbell, G.C.; Bartley, W.J.; Johnson, J.H. Rhenium and its compounds as hydrogenation catalysts. III. rhenium heptoxide. *J. Org. Chem.* **1959**, *24*, 1847–1854. [CrossRef]
47. Mao, B.W.; Cai, Z.Z.; Huang, M.Y.; Jiang, Y.Y. Hydrogenation of carboxylic acids catalyzed by magnesia-supported poly-γ-aminopropylsiloxane-Ru complex. *Polym. Adv. Technol.* **2003**, *14*, 278–281. [CrossRef]
48. Jones, R.V.; Godorhazy, L.; Varga, N.; Szalay, D.; Urge, L.; Darvas, F. Continuous-flow high pressure hydrogenation reactor for optimization and high-throughput synthesis. *J. Comb. Chem.* **2006**, *8*, 110–116. [CrossRef] [PubMed]